Journal of New Materials for Electrochemical Systems 17, 129-132 (2014)

Impedance Analysis of Growth and Morphology of Electropolymerized Polypyrrole Nanocomposites

Morteza Torabi[1,2], M. Soltani[3,4] and S.K. Sadrnezhaad[1,*]

[1]Materials and Energy Research Center, P.O. Box 14155-4777, Tehran, Iran
[2]University of Waterloo, N2L 3G1,Waterloo, ON, Canada
[3]KNT University of Technology , P.O. Box 15875-4416, Tehran, Iran
[4]Johns Hopkins University, Baltimore, Maryland 21218, USA

Received: February 24, 2013, Accepted: April 22, 2014, Available online: April 24, 2014

Abstract: *Pure polypyrrole (PPy), PPy/Al_2O_3 and PPy/SiO_2 nanocomposites synthesized galvanostatically using different polymerization charges. Electrochemical impedance measurements of pure polypyrrole revealed that the film thickness affected the impedance responses. The characteristic frequencies vs. film thickness that obtained using Cole-Cole plots showed that electrodeposition mechanism changed from 3D to 1D after nuclei overlapping for pure PPy. Analysis of the nanocomposites impedance spectrums revealed no changes during the film growth, i.e. deposition continues 3D even after nuclei overlapping. Scanning electron microscopy (SEM) confirmed the impedance results and showed that the morphology of the thick pure PPy film is 1D, while the deposition of the nanocomposites was 3D with compact and very fine structure.*

Keywords: Electrochemical impedance spectroscopy; Conducting polymers; Characteristic frequency; Nanocomposite; Cole-Cole plots

1. INTRODUCTION

Conductive polymers such as polypyrrole, polyaniline and polythiophene are important classes of polymers [1-4], since ionic substances could be incorporated into and released from them easily and repeatedly.

Both electron and ion transport within these polymers occur during doping (conducting) and undoping (nonconducting) processes. These mass and charge transport processes are fundamental to many applications [5-8] and thus, intensive researches were focused on the switching process in conducting polymers. It is often found that ion transport is slower than the electron transport and therefore, it limits the switching rate. The rate controlling factor for low-frequency processes depends mainly on the chemical diffusion coefficient (D) and the diffusion length (l) [9]. When the diffusion is limiting process these two parameters determine the rate of doping through following equation:

$$\omega_d = \frac{D}{l^2} \quad (1)$$

There are a few problems with the use of potential step techniques to measure ion diffusion coefficients in polymer films [15]. As known, impedance spectroscopy is a common method to determine ω_d experimentally [9].

On the other hand, the morphology of the electrochemically synthesized conducting polymers depends on deposition conditions [10]. In all, when the film thickness of the polymer is less than 100 nm, ordered and homogeneous structures are developed [9]. After growing of this homogeneous structure, porous film will be formed which is depending on the deposition rate and the used counterion [9].

Meanwhile, in order to achieve a new function of PPy, one of the most efficient methods is to prepare PPy-based composite films where new chemical components, such as nanoparticles of Fe_2O_3 [11] and Pd [12] or nanostructure clays [13, 14], are introduced. Compact morphology of the PPy nanocomposites will shows different physical and chemical properties respect to the

*To whom correspondence should be addressed:
Email: sadrnezh@sharif.edu
Phone: +98 261 6210009, Fax: +98 261 6201877

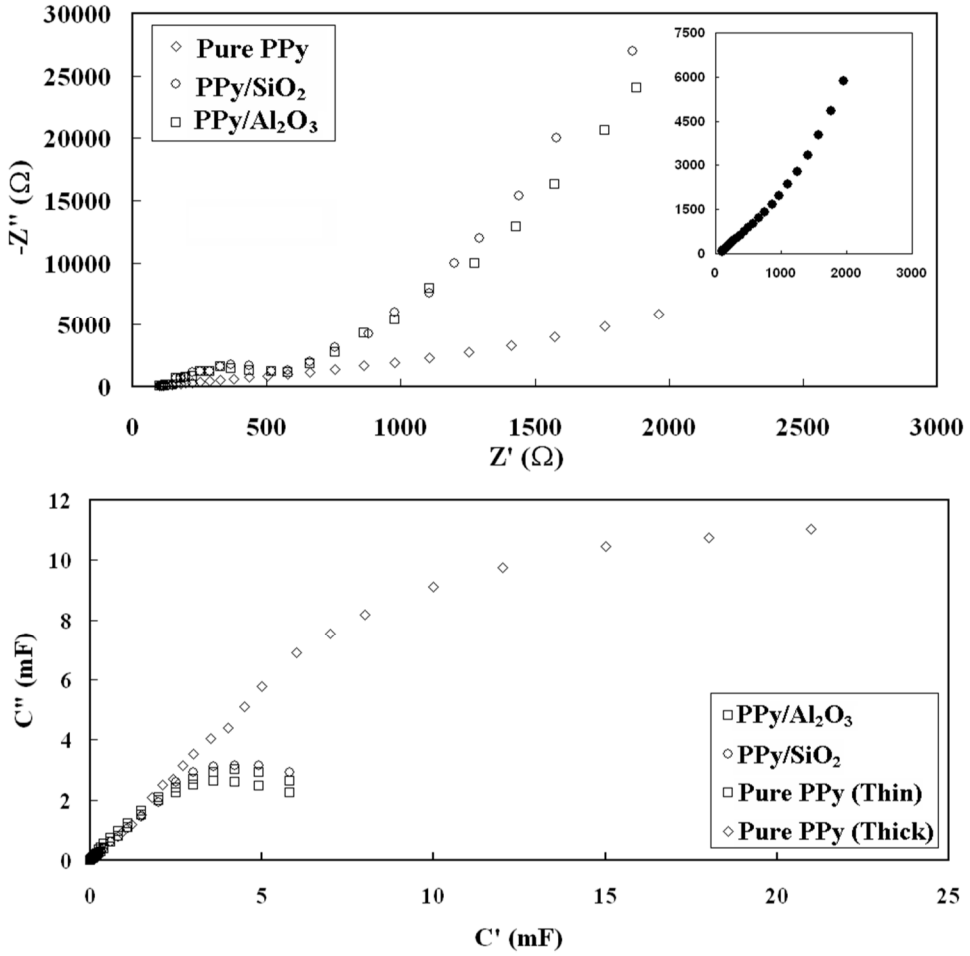

Figure 1. (a) Complex plane impedance plots for pure PPy, PPy/Al_2O_3 and PPy/SiO_2 nanocomposites and (b) complex capacitance plots.

pure PPy [19]. Therefore, PPy nanocomposites structure and growth model are very important for their properties.

In this paper, the influence of electrode structure on the kinetics of diffusion process in the pure PPy and PPy nanocomposites was studied by analyzing the capacitive response observed at low frequencies.

2. EXPERIMENTAL

Alumina and silica nanoparticles were obtained from Sigma-Aldrich, US. The other chemical reagents used in this work were purchased from MERCK, Germany. Polypyrrole films were electropolymerized galvanostatically (0.2 mA cm^{-2}) onto Pt sheet using 0.1 M pyrrole and 0.1 M $LiClO_4$ in aqueous solution. As Bull et al. [16] reported, thickness growth rate is approximately 2 μm C^{-1} cm^2, different films were grown from ~20 nm up to ~300 nm. The obtained films transferred to an aqueous solution of 0.1 M $LiClO_4$ for electrochemical impedance tests. The polymeric films deposited onto the Pt were the working electrodes. Pt rod and Ag/AgCl electrode were used as counter and reference electrodes. The electrochemical impedance measurements performed in the frequency range from 100 kHz down to 0.1 mHz, using an ac voltage of 10 mV rms at different dc potentials. All electrochemical synthesis and EIS investigations were performed using Autolab PGSTAT30 equipment with frequency analyzer module. Surface morphology of the coatings, were investigated by scanning electron microscopy (SEM, Philips XL30).

3. RESULTS AND DISCUSSION

The Nyquist plots for pure PPy/ ClO_4^- , PPy/Al_2O_3, and PPy/SiO_2 nanocomposites at 0.2 V vs. Ag/AgCl are presented in Fig. 1a. The real axis intercept at high frequency is independent of the electrode material for all cases. This intercept coincides with the uncompensated resistance of the bulk electrolyte solution (R_s≈90Ω). Therefore, it can be concluded that the ionic or the electronic resistance of the polymer is very small with respect to the solution resistance. Therefore, charge transfer in all films is fast when they are oxidized. The redox reaction starts at polymer/solution interface at high frequencies and with decreasing the frequency, Warburg line with slope about 45° revealed in the impedance spectrum. So, the redox reaction layer grows into the polymer from the polymer/solution interface. At lower frequencies, an almost vertical line was revealed in the spectrum, i.e. the redox reaction layer includes the polymeric film and the polymer-coated

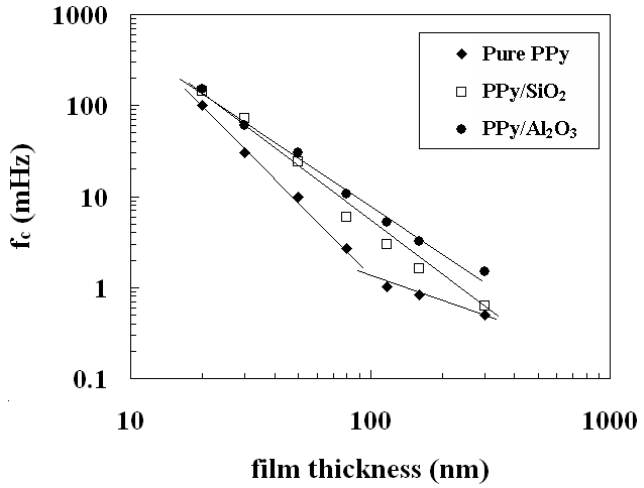

Figure 2. Characteristic frequency of the diffusion process $f_d=\omega_d/2\pi$ (Eq. (1)) calculated from the capacitance plots at 0.2 V *vs.* Ag/AgCl under variation of the polymerization charge.

electrode behaves like a simple capacitor. Such spectrum can be modeled with a finite transmission line circuit [17, 18]. The ionic resistances of the coatings can be obtained using following equation:

$$R_{ion} = 3(R_{low} - R_s) \tag{2}$$

where R_{low} is the real axis intercept of the vertical line at low frequency region of the spectrum. Then, the ionic conductivity of the film (σ_{ion}) is calculated from the Eq. (3):

$$\sigma_{ion} = \frac{d}{R_{ion} A} \tag{3}$$

where A is the electrode surface and d is the film thickness.

These results are presented in Table 1 for pure PPy and the nanocomposites for thickness of about 100 nm. As it can be seen in the Table 1, the ionic resistance and ionic conductivity of the nanocomposites are the same as the pure PPy since ClO_4^- was used as doping anion in all experiments.

As reported in the literature [17, 18] it is useful to describe the low-frequency wing of the spectra in terms of capacitance plots. This procedure was performed for coated electrodes at various polymerization charges and results are observed at Fig. 1b for pure PPy and the nanocomposites. Two separated patterns are observed

Table 1. Low frequency resistance, ionic resistance and ionic conductivity of the pure PPy and the PPy nanocomposites (film thickness (d) = 100 nm, electrode surface (A) =1 cm^2).

	R_s (Ω)	R_{ion} (Ω)	σ_{ion} (G Ω^{-1} cm^{-1})
Pure PPy	87	1085	9.217
PPy/Al_2O_3	95	1095	9.132
PPy/SiO_2	93	1091	9.166

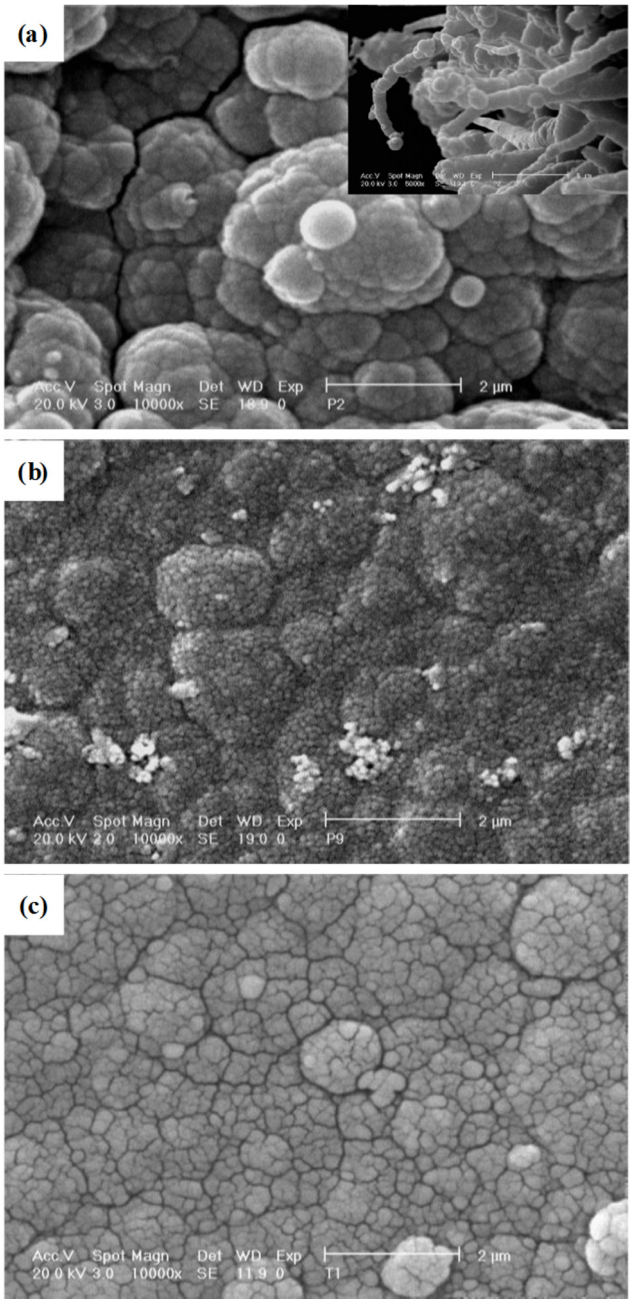

Figure 3. SEM results of the polymeric films deposited using 280 $mCcm^{-2}$; (a) pure PPy, (b) PPy/Al_2O_3 and (c) PPy/SiO_2 nanocomposite.

for low polymerization charges of pure PPy; an ~45°-inclined line at high frequencies and a single semicircle at intermediate and low frequency. On the other hand, for high polymerization charges, the relaxational behavior dominates the whole plot. For nanocomposites, no considerable changes were observed in the Cole-Cole plots at various polymerization charges and the behavior of the high polymerized nanocomposites is the same as the low polymerization charges.

The characteristic frequency of diffusion ω_d ($f_d = \frac{\omega_d}{2\pi}$) can be found from the maximum point of the imaginary part of the capacitance [18]. Fig. 2 shows dependence of characteristic frequency to polymerization charge Q for pure PPy and the nanocomposites. In log-log plane, the dependency of the diffusion characteristic frequency to the film thickness is linear with relation of $f_d \propto L^{-\gamma}$. This dependency is much stronger for thin pure PPy and nanocomposites with a calculated γ exponent near to one. With comparison of these results with Eq. (1), it is obvious that $l \approx L$. In contrast, with increasing the polymerization charge and therefore thickness of the pure PPy, the dependency of the f_d with the thickness of the film is weaker and so $l \ll L$. As discussed in [17], with initiation of growing the porous structure of the films, the growth mechanism is changed from 3D to 1D for pure PPy. At transient point (80 mC cm^{-2}), with growing and encountering nucleus, the porous structure is deposited and after nuclei overlapping, the growth continues perpendicular to the macroscopic interface [17].

In contrast to the pure PPy, there is no transition point at the Cole-Cole plots of the nanocomposite. Therefore, it can be concluded that the nanocomposite growth occurred in 3D after overlapping the nuclei. It is demonstrated previously that [19] the addition of the nanoparticles leads to a catalytic effect and formed an electroxidation pathway for the polymerization of the PPy. Furthermore, adsorption of the nanoparticles on the surface inhibited 1D growth.

SEM images of pure PPy and the nanocomposites presented in Fig. 3, confirmed the above results about the nucleation and growth mechanisms which are found from Cole-Cole plots. While, Garcia-Belmonte [9] reported that the thick PPy films are more porous than the thinner one, only PPy and nanocomposites synthesized at high polymerization charges are presented here. Fig. 3a showed that the pure PPy structure is porous and 1D growth of the PPy is so clear. But, the SEM results of the morphology of the nanocomposites at Fig. 3b and 3c revealed that the nanocomposite growth is 3D and a compact morphology is obtained.

4. CONCLUSION

Electrochemical impedance spectroscopy of pure PPy and PPy nanocomposites were used in order to investigate the slow ionic diffusion of the counterion into the films with use of Cole-Cole plots. The behavior was significantly different for thick pure PPy films which were synthesized at higher polymerization charge which contained a drastic change in the dependency of the characteristic frequency to the film thickness at about 80 nm. Increasing of the film thickness for pure PPy, results in the growth mechanism change from 3D to 1D and also rough and porous morphology formation. In contrast, the electrode morphology is compact and homogeneous and deposition continued its 3D structure during the electropolymerization of the pyrrole in the presence of alumina and silica nanoparticles.

REFERENCES

[1] A.F. Diaz, K.K. Kanazawa, G.P. Gardini, J. Chem. Soc. Chem. Commun., 14, 635 (1979).

[2] K.K. Kanazawa, A.F. Diaz, B.H. Geiss, W.D. Gill, J.F. Kwark, J.A. Logan, J.F. Rabolt, G.B. Street, J. Chem. Soc. Chem. Commun., 19, 854 (1979).

[3] A. Watanabe, M. Tanaka, J. Bull. Chem. Soc. Jpn., 54, 2278 (1981).

[4] J.L. Bredas, R. Silbey, D.S. Boudreaux, R.R. Chance, J. Am. Chem. Soc., 105, 6555 (1983).

[5] A.F. Diaz, J.F. Rubinson, H.B. Mark, J. Adv. Polym. Sci., 84, 113 (1988).

[6] M. Kaneko, D. Wohrle, Adv. Polym. Sci., 84, 141 (1988).

[7] M.G. Kanatzidis, Chem. Eng. News, 68, 36 (1990).

[8] A. Techagumpuch, H.S. Nalwa, S. Miyata, *in* "Electroresponsive Molecular and Polymeric Systems", Ed., T.A. Skotheim, Marcel Decker, New York, USA, 1991, p. 257.

[9] Germà Garcia-Belmonte, Electrochem. Commun., 5, 236 (2003).

[10]E.L. Kupila, J. Kankare, Synth. Met., 74, 241 (1995).

[11]P. Zhang, Z.H.Yang, D.J. Wang, S.H. Kan, X.D. Chai, J.Z. Liu, T.J. Li, Synth. Met., 84, 165 (1997).

[12]N. Cioffi, L. Torsi, L. Sabbatini, P.G. Zambonin, T.B. Zacheo, J. Electroanal. Chem., 488, 42 (2000).

[13]S. Sinharay, M. Biswas, Mater. Res. Bull., 34, 1187 (1999).

[14]K. Ramachandran, M.M. Lerner, J. Electrochem. Soc., 144, 3739 (1997).

[15]X. Ren, P.G. Pickup, J. Phys. Chem., 97, 5356 (1993).

[16]R.A. Bull, F.R.F. Fan, A.J. Bard, J. Electrochem. Soc., 129, 1009 (1982).

[17]G. Garcia-Belmonte, J. Bisquert, Electrochim. Acta, 47, 4263 (2002).

[18]X. Ren, G. Pickup, J. Phys. Chem., 97, 5356 (1993).

[19]Y.C. Liu, C.J. Tsai, J. Electroanal. Chem., 537, 165 (2002).